Conf-920375--24

Prediction of Aging Degradation of Cast Stainless Steel Components in LWR Systems*

O. K. Chopra

Materials and Components Technology Division
Argonne National Laboratory
9700 South Cass Avenue
Argonne, Illinois 60439 USA

ANL/CP--75791

DE92 014848

U 4 1992

March 1992

Presented at NRC Aging Research Information Conference, March 24–27, 1992, Rockville, MD.

*Work supported by the office of Nuclear Regulatory Research, U.S. Nuclear Regulatory Commission, FIN No. A22432; Project Manager: J. Muscara.

Prediction of Aging Degradation of Cast Stainless Steel Components in LWR Systems*

Omesh K. Chopra

Materials and Components Technology Division
Argonne National Laboratory
9700 South Cass Avenue
Argonne, Illinois 60439 USA

Abstract

A procedure and correlations are presented for predicting Charpy-impact energy, tensile flow stress, fracture toughness J–R curve, and J_{IC} of aged cast stainless steels from known material information. The "saturation" impact strength and fracture toughness of a specific cast stainless steel, i.e., the minimum value that would be achieved for the material after long-term service, is estimated from the chemical composition of the steel. Mechanical properties as a function of time and temperature of reactor service are estimated from impact energy and flow stress of the unaged material and the kinetics of embrittlement, which are also determined from chemical composition. The J_{IC} values are determined from the estimated J–R curve and flow stress. Examples of estimating mechanical properties of cast stainless steel components during reactor service are presented. A common "predicted lower-bound" J–R curve for cast stainless steels of unknown chemical composition is also defined for a given grade of steel, ferrite content, and temperature.

1 Introduction

Cast stainless steels used in light water reactor (LWR) systems for primary pressure-boundary components such as valve bodies, pump casings, and primary coolant piping are susceptible to thermal embrittlement at reactor operating temperatures, i.e., 280–320°C. Thermal aging of cast stainless steels at these temperatures increases hardness and tensile strength and decreases ductility, impact strength, and fracture toughness of the material. The Charpy transition curve shifts to higher temperatures. Investigations at Argonne National Laboratory (ANL)[1-4] and elsewhere[5-11] have shown that thermal embrittlement of cast stainless steels can occur during the reactor design lifetime of 40 y. Different grades and heats exhibit different degrees of embrittlement. In general, the low-carbon CF-3 steels are the most resistant to thermal embrittlement and the Mo-bearing high-carbon CF-8M steels are the least resistant. The extent of thermal embrittlement increases with increased ferrite content.

Thermal aging of cast stainless steels at <500°C leads to precipitation of additional phases in the ferrite, e.g., formation of a Cr-rich α' phase by spinodal decomposition; nucleation and growth of α'; precipitation of a Ni- and Si-rich G phase, $M_{23}C_6$, and γ_2; and additional precipitation and/or growth of existing carbides at the ferrite/austenite phase boundaries.[12-18] The formation of Cr-rich regions by spinodal decomposition is the primary strengthening mechanism for ferrite, which increases strain-hardening and local tensile

* Work supported by the office of Nuclear Regulatory Research, U.S. Nuclear Regulatory Commission, FIN No. A22432; Project Manager: J. Muscara.

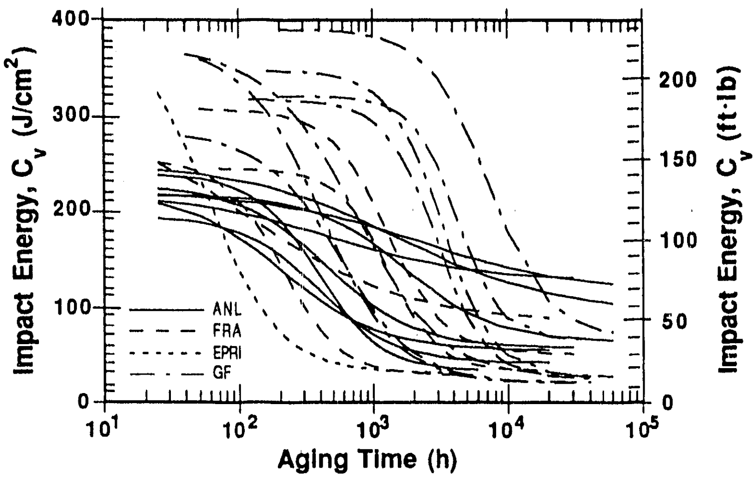

Figure 1. Decrease in Charpy-impact energy for various heats of cast stainless steels aged at 400°C

stress. Consequently, the critical stress for brittle fracture, i.e., either cleavage of the ferrite or separation of the ferrite/austenite phase boundary, is achieved at higher temperatures.

The degree or extent of thermal embrittlement is controlled by the amount of brittle fracture. A predominantly brittle failure occurs when either the ferrite phase is continuous, e.g., in cast material with a large ferrite content, or the ferrite/austenite phase boundary provides an easy path for crack propagation, e.g., in high-C or high-N steels that contain phase-boundary carbides or nitrides. Consequently, the amount, size, and distribution of the ferrite in the duplex structure and phase-boundary precipitates are important parameters that control the extent of thermal embrittlement.

Current assessments of thermal embrittlement of cast stainless steels involve simulation of end-of-design-life reactor conditions by accelerated aging at higher temperatures, viz., 400°C, because the time period for operation of power plants (≈40 y) is far longer than can generally be considered for laboratory studies. Estimates of mechanical-property degradation of cast stainless steel components are based on an Arrhenius extrapolation of high-temperature data to reactor operating conditions.

The temperature dependence of thermal embrittlement is controlled primarily by the kinetics of ferrite strengthening, i.e., the size and spacing of Cr fluctuations produced by spinodal decomposition of ferrite. Small changes in the constituent elements of the material can cause the kinetics of thermal embrittlement to vary significantly. Activation energies of thermal embrittlement can range from 65 to 230 kJ/mole. Also, the aging behavior at 400°C shows significant heat-to-heat variation. The decrease in Charpy-impact energy during thermal aging at 400°C for various heats of cast stainless steels[3-5,9,11] is shown in Fig. 1. The results indicate that all materials reach a "saturation" impact energy, i.e., minimum value that would be achieved by the material after long-term aging. Saturation impact energy, in general, decreases with an increase in ferrite content or the concentration of C or N in the steel; both of these factors promote brittle fracture.

Figure 1 also indicates that the time for aging at 400°C for a given decrease in impact energy varies more than 2 orders of magnitude for the various heats. Production heat treatment, and possibly the casting process, influence aging behavior at 400°C and, therefore, the kinetics of thermal embrittlement. The log of the aging time at 400°C for a 50%

reduction in Charpy-impact energy has been shown to be a useful parameter for characterizing the kinetics of thermal embrittlement.[19] Activation energy for thermal embrittlement is high for steels that show fast embrittlement at 400°C and low for those that show slow embrittlement at 400°C.

A procedure and correlations have been developed for estimating mechanical properties of cast stainless steel components under LWR operating conditions.[19] These correlations have recently been optimized with data on materials that were aged up to ≈55,000 h at 290–350°C.[20] The analysis focused on developing correlations for fracture properties in terms of material information in certified material test records (CMTRs) and on ensuring that the estimated mechanical properties are adequately conservative for cast stainless steels defined by ASTM Specification A 351. The correlations do not consider the effect of metallurgical differences that may arise from differences in production heat treatment or casting process and, therefore, may be conservative for some steels. This paper describes the procedure for estimating Charpy-impact, tensile flow stress, and fracture toughness of cast stainless steels during thermal aging in LWRs.

2 Procedure for Estimating Mechanical Properties

Mechanical properties of a specific cast stainless steel are estimated from the extent and kinetics of thermal embrittlement. The extent of thermal embrittlement is characterized by room-temperature (RT) "normalized" Charpy-impact energy. A correlation for the extent of embrittlement at "saturation" is given in terms of chemical composition. Extent of thermal embrittlement as a function of time and temperature of reactor service is estimated from the extent of embrittlement at saturation and from the correlations describing the kinetics of embrittlement, which are also given in terms of the chemical composition of the steel. The fracture toughness J-R curve for the material is then obtained from the correlation between fracture toughness parameters and the RT Charpy-impact energy used to characterize the extent of thermal embrittlement. Tensile flow stress is estimated from initial flow stress of the unaged material and the kinetics of thermal embrittlement. Fracture toughness J_{IC} and tearing modulus can then be determined from the estimated J-R curve and tensile flow stress. A common lower-bound J-R curve for cast stainless steels of unknown chemical composition is also defined for a specific grade of steel, range of ferrite content, and temperature.

A flow diagram for estimating mechanical properties of cast stainless steels during reactor service is shown in Fig. 2. The estimation scheme is divided into three sections on the basis of available material information. In Section A, "predicted lower-bound" fracture toughness and Charpy-impact energy are defined for CF-3, CF-8, and CF-8M steels of unknown chemical composition. The cast stainless steels used in the U.S. nuclear industry generally contain <15% ferrite. The lower-bound mechanical properties for a specific grade of steel are based on the "worst case" chemical composition (>15% ferrite) and are thus very conservative for most steels. More realistic estimates of lower-bound properties can be obtained if the ferrite content of the steel is known. Different lower-bound J-R curves and impact energy are defined for steels containing <10%, 10–15%, or >15% ferrite.

Sections B and C of Fig. 2 present procedures for estimating mechanical properties when CMTR is available. Section B describes the estimation of "saturation" impact energy and fracture toughness J-R curve. The only information needed for these estimations is the chemical composition of the material. The present correlations account for the degradation of mechanical properties due to thermal aging. They do not explicitly consider the initial

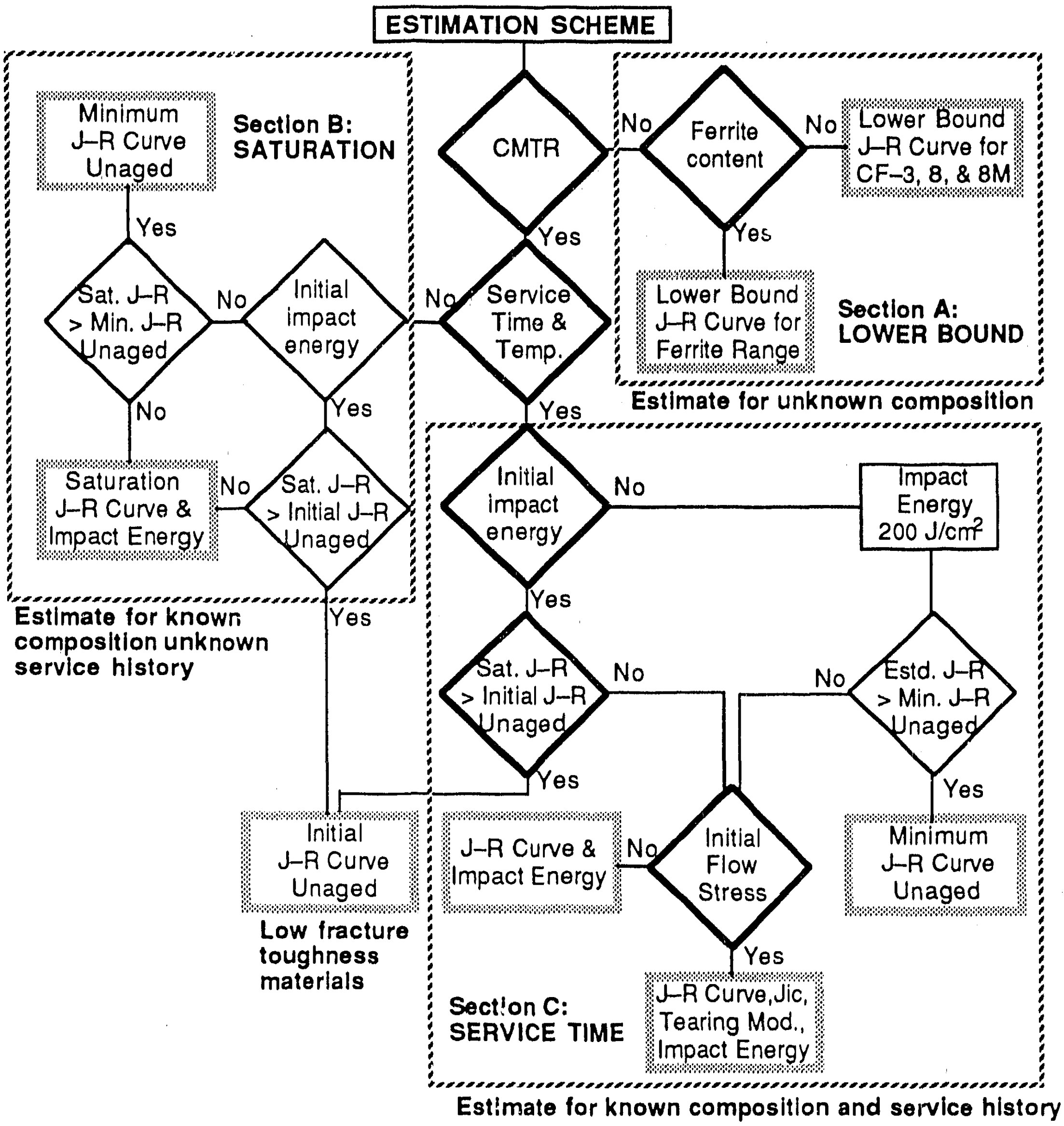

Figure 2. Flow diagram for estimating mechanical properties of aged cast stainless steels in LWR systems

fracture properties of the original unaged material. To take this into account, estimated saturation J–R curves are used only when they are lower than the minimum J–R curve of unaged cast stainless steels or J–R curve of the unaged material, if known. When no information is available on the initial fracture toughness or initial RT Charpy impact energy for estimating fracture toughness of a material, and when the J–R curve estimated from the chemical composition is higher than the minimum fracture toughness of unaged cast stainless steels, the latter is used as the saturation J–R curve of a material. Furthermore, some cast stainless steels are inherently weak and may have poor fracture properties in the unaged condition. Estimations of saturation fracture toughness based on chemical composition may be higher than the fracture toughness of the unaged material. Such cases indicate no thermal aging effects, and thus the fracture toughness of the material would not change during reactor service.

Estimation of mechanical properties at any given time and temperature of service is described in Section C of Fig. 2. The initial impact energy and flow stress of the unaged material are required for these estimations. The J_{IC} value and tearing modulus are determined from the estimated J-R curve and flow stress. The initial impact energy can be assumed to be 200 J/cm^2 if not known. However, similar to Section B, when the estimated fracture toughness is higher than the minimum fracture toughness of unaged cast stainless steels, the latter is used as the estimated fracture toughness of a material after service. Also, some cast stainless steels may not show any thermal aging effects.

3 Predicted Lower-Bound Fracture Toughness

For cast stainless steels of unknown chemical composition, lower-bound fracture toughness is defined for a given material grade and temperature. For cast stainless steels within ASTM Specification A 351, the saturation RT impact energy can be as low as 30, 25, and 20 J/cm^2 for CF-3, CF-8, and CF-8M steels, respectively. The lower-bound J-R curves at RT and 290°C for static- and centrifugally cast CF-3, CF-8, and CF-8M are shown in Figs. 3 and 4. These lower-bound J-R curves are for steels containing >15% ferrite and are

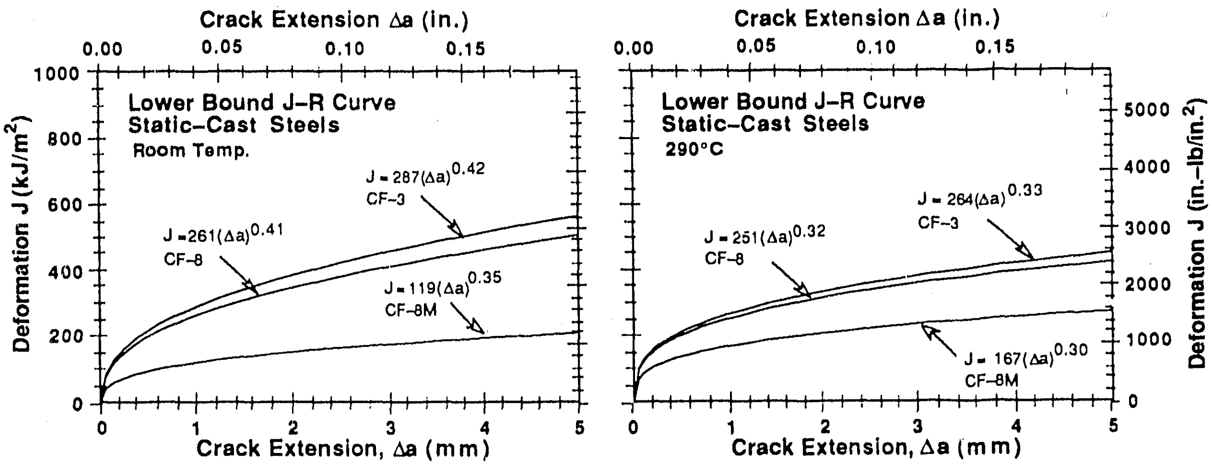

Figure 3. Lower bound J-R curve for static-cast stainless steels

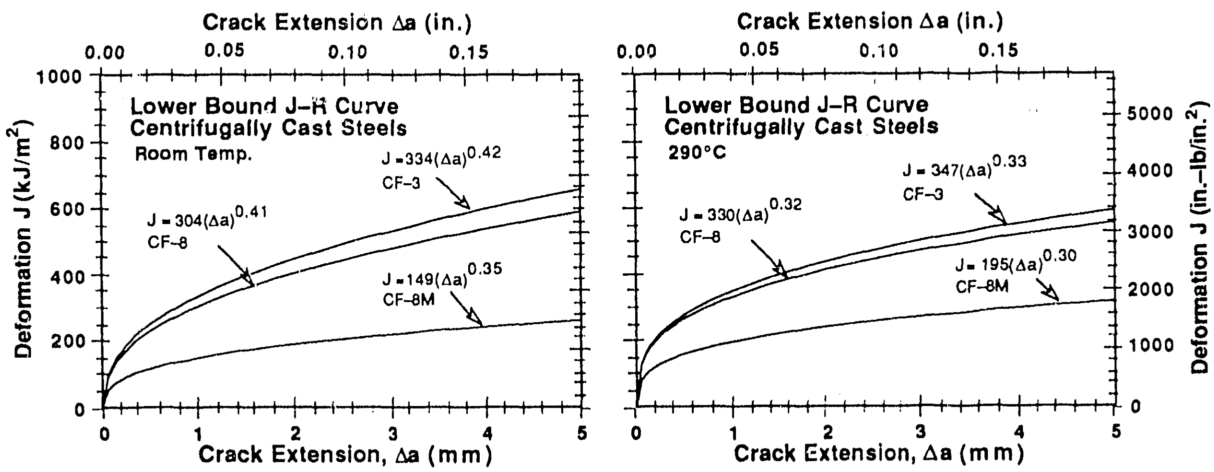

Figure 4. Lower bound J-R curve for centrifugally cast stainless steels

Table 1. Values of the coefficient C and exponent n for the lower-bound J-R curve for cast stainless steels

			Static-Cast				Centrifugally Cast			
		Cv	Room Temp.		290°C		Room Temp.		290°C	
Grade	φ	(J/cm²)	C	n	C	n	C	n	C	n
Ferrite Content >15%										
CF-3	40	30	287	0.42	264	0.33	334	0.42	347	0.33
CF-8	48	25	261	0.41	251	0.32	304	0.41	330	0.32
CF-8M	40	20	119	0.35	167	0.30	149	0.35	195	0.30
Ferrite Content 10-15%										
CF-3	30	42	342	0.45	290	0.35	398	0.45	382	0.35
CF-8	36	34	307	0.42	274	0.33	357	0.43	360	0.33
CF-8M	32	28	149	0.36	192	0.31	186	0.36	223	0.31
Ferrite Content <10%										
CF-3	20	67	400	0.47	331	0.38	507	0.50	435	0.38
CF-8	24	55	394	0.46	313	0.35	458	0.46	412	0.35
CF-8M	24	47	211	0.38	238	0.33	264	0.38	276	0.33

thus very conservative for most steels used in the U.S. nuclear industry. The ferrite content of a cast stainless steel component can be measured in the field with a ferrite scope and a remote probe. The values of the coefficient C and exponent n representing the lower-bound J-R curve for aged cast stainless steels with >15%, 10–15%, and <10% ferrite are given in Table 1. This information may be used as a guideline for establishing the upper limit of ferrite content for each grade of steel beyond which thermal aging effects are significant.

4 Mechanical Properties at Saturation

4.1 Charpy-Impact Energy

The variation of this saturation impact energy Cv_{sat} for different materials can be expressed in terms of a material parameter Φ that is determined from the chemical composition and ferrite content of the materials. The ferrite content is calculated in terms of the Hull's equivalent factors[21]

$$Cr_{eq} = Cr + 1.21(Mo) + 0.48(Si) - 4.99 \quad (1)$$

and

$$Ni_{eq} = (Ni) + 0.11(Mn) - 0.0086(Mn)^2 + 18.4(N) + 24.5(C) + 2.77. \quad (2)$$

The concentration of N is often not available in the CMTR; if not known, it is assumed to be 0.04 wt.%. The ferrite content δ_c is given by

$$\delta_c = 100.3(Cr_{eq}/Ni_{eq})^2 - 170.72(Cr_{eq}/Ni_{eq}) + 74.22. \quad (3)$$

Different correlations are used to estimate the saturation impact energy of the various grades of cast stainless steel. For CF-3 and CF-8 steels, the material parameter Φ is expressed as

$$\Phi = \delta_c(Cr + Si)(C + 0.4N), \quad (4)$$

and the saturation value of RT impact energy Cv_{sat} is given by

$$\log_{10}Cv_{sat} = 1.15 + 1.36\exp(-0.035\Phi). \quad (5)$$

For the Mo-bearing CF-8M steels, the material parameter Φ is expressed as

$$\Phi = \delta_c(Ni + Si + Mn)^2(C + 0.4N)/5. \quad (6)$$

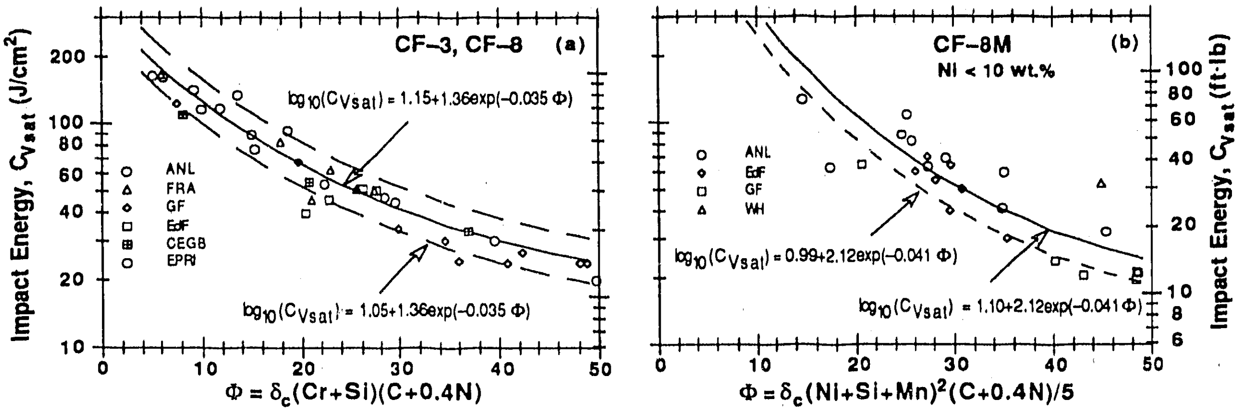

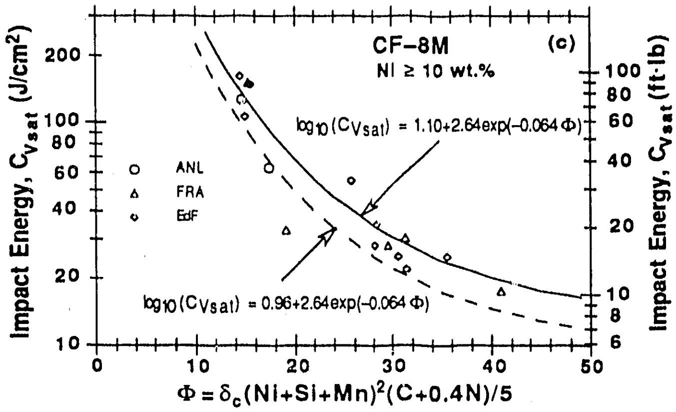

Figure 5.
Correlation between RT Charpy-impact energy at saturation and material parameter for CF-3, CF-8, and CF-8M steels

The saturation value of RT impact energy Cv_{sat} for steels with <10% Ni is given by

$$\log_{10}Cv_{sat} = 1.10 + 2.12\exp(-0.041\Phi), \tag{7}$$

and for steels with >10% Ni by

$$\log_{10}Cv_{sat} = 1.10 + 2.64\exp(-0.064\Phi). \tag{8}$$

The N content in Eqs. 4 and 6 can be assumed to be 0.04 wt.% if the value is not known. The RT saturation impact energy is also estimated from the chemical composition of the steel. For CF-3 and CF-8 steels, Cv_{sat} is given by

$$\log_{10}Cv_{sat} = 5.64 - 0.006\delta_c - 0.185Cr + 0.273Mo - 0.204Si + 0.044Ni - 2.12(C + 0.4N), \tag{9}$$

and for CF-8M steels by

$$\log_{10}Cv_{sat} = 7.28 - 0.011\delta_c - 0.185Cr - 0.369Mo - 0.451Si - 0.007Ni - 4.71(C + 0.4N). \tag{10}$$

The saturation impact energy for a specific cast stainless steel is determined by both the methods given in Eqs. 4–10, and the lower of the two values is used for estimating mechanical properties.

The saturation values of RT impact energy for CF-3, CF-8, and CF-8M steels predicted by Eqs. 4–8 and those observed experimentally at ANL,[3,4,12,13] GF,[5] Westinghouse (WH),[6] Electricité de France (EdF),[7] Central Electricity Generation Board (CEGB),[8] FRA,[9] and EPRI[11] are shown in Fig. 5. The difference between observed and predicted values for the

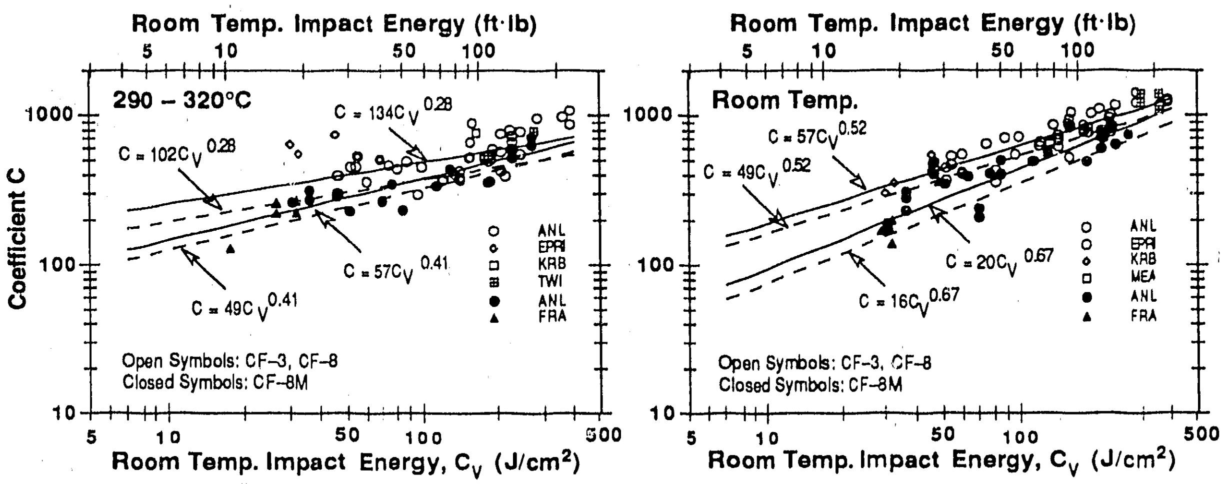

Figure 6. Correlation between RT Charpy-impact energy and coefficient C at 290–320°C and room temperature. The solid and dashed lines represent the correlations used to estimate the J-R curves for centrifugally and static-cast materials, respectively.

CF-8M steel is larger than that for the CF-3 or CF-8 steels. The correlations expressed in Eqs. 4–10 do not include Nb, and may not be conservative for Nb-bearing steels.

4.2 Fracture Toughness

The saturation fracture toughness J-R curve for a specific cast stainless steel can be estimated from its RT impact energy at saturation. The J-R curve is expressed by the power-law relation $J_d = C\Delta a^n$. The coefficient C at room and reactor temperatures and the RT Charpy-impact energy C_V for aged and unaged cast stainless steels are plotted in Fig. 6. Fracture toughness data from ANL,[3,4,12,13] FRA,[9,10] EPRI,[11] Materials Engineering Associates (MEA),[22] and The Welding Institute (TWI)[23] studies are included in the figure. At both temperatures, the coefficient C decreases with a decrease in impact energy. Separate correlations were obtained for CF-3 or CF-8 steels and for CF-8M steels; the latter showed a larger decrease in fracture toughness for a given impact energy. The correlations used to estimate J-R curves for static-cast materials were obtained by subtracting the value of σ from the best-fit curve. They are shown as dashed lines in Fig. 6, and help ensure that the estimated J-R curve is conservative for all material and aging conditions. Best-fit correlations were used for centrifugally cast materials. The saturation fracture toughness J-R curve at RT for static-cast CF-3 and CF-8 steels is given by

$$J_d = 49[C_V]^{0.52}[\Delta a]^n, \quad (11)$$

and for static-cast CF-8M steels by

$$J_d = 16[C_V]^{0.67}[\Delta a]^n. \quad (12)$$

At 290-320°C, the J-R curve for static-cast CF-3 and CF-8 steels is given by

$$J_d = 102[C_V]^{0.28}[\Delta a]^n, \quad (13)$$

and for static-cast CF-8M steels by

$$J_d = 49[C_V]^{0.41}[\Delta a]^n. \quad (14)$$

Table 2. Constants in Eq. 15 for estimating exponent n of the power–law J–R curve

	Room Temp.		290–320°C	
Grade	a_2	b_2	a_2	b_2
CF–3	0.08	0.228	0.14	0.130
CF–8	0.22	0.139	0.22	0.074
CF–8M	0.25	0.077	0.23	0.057

For centrifugally cast steels, the constants in Eqs. 11–14 are 57, 20, 134, and 57, respectively. At RT, the exponent n for static– or centrifugally cast steels is given by

$$n = a_2 + b_2 \log_{10} C_V, \tag{15}$$

where the values of the constants a_2 and b_2 for different grades of steel and test temperature are given in Table 2. The J–R curve at any intermediate temperature can be linearly interpolated from the estimated values of C and n at RT and at 290°C.

The fracture toughness J–R curve at saturation for a specific cast stainless steel can be obtained from its chemical composition using the correlations for C_{Vsat} given in Eqs. 1–10 and then using this estimated C_{Vsat} for C_V in Eqs. 11–14 to obtain the J–R curve. Comparisons of the experimental and estimated J–R curves at saturation, i.e., the minimum fracture toughness that would be achieved for the material by thermal aging, are shown in Fig. 7. The experimental and estimated J–R curve for the unaged materials are also shown for comparison; the J–R curves were estimated using the measured initial RT impact energy C_{Vint}. The estimated curves show good agreement with the experimental results in most cases and are essentially conservative. The estimated J–R curve after 32 effective full power years (efpy) of service at 320°C is also shown in Fig. 7. The results indicate that for 320°C service, fracture toughness of these materials will reach the saturation value or will be close to saturation within the 40–y design life.

When no information is available on the initial fracture toughness of a specific material, the minimum fracture toughness of unaged cast stainless steels is used as upper bound for the predicted fracture toughness of the aged material. At temperatures between RT and 320°C, the minimum fracture toughness of unaged static–cast stainless steels can be expressed as[19]

$$J_d = 400[\Delta a]^{0.40} \tag{16}$$

and of centrifugally cast stainless steels as

$$J_d = 650[\Delta a]^{0.43}. \tag{17}$$

Equation 16 or 17 is used when the J–R curve predicted by Eqs. 11–14 is higher than that given by Eq. 16 or 17.

5 Service Time Properties

5.1 Kinetics of Thermal Embrittlement

Room–temperature impact energy as a function of time and temperature of aging is estimated from the RT saturation impact energy C_{Vsat} and the kinetics of embrittlement. The decrease in RT Charpy–impact energy C_V with time is expressed as

$$\log_{10} C_V = \log_{10} C_{Vsat} + \beta\{1 - \tanh[(P - \theta)/\alpha]\}. \tag{18}$$

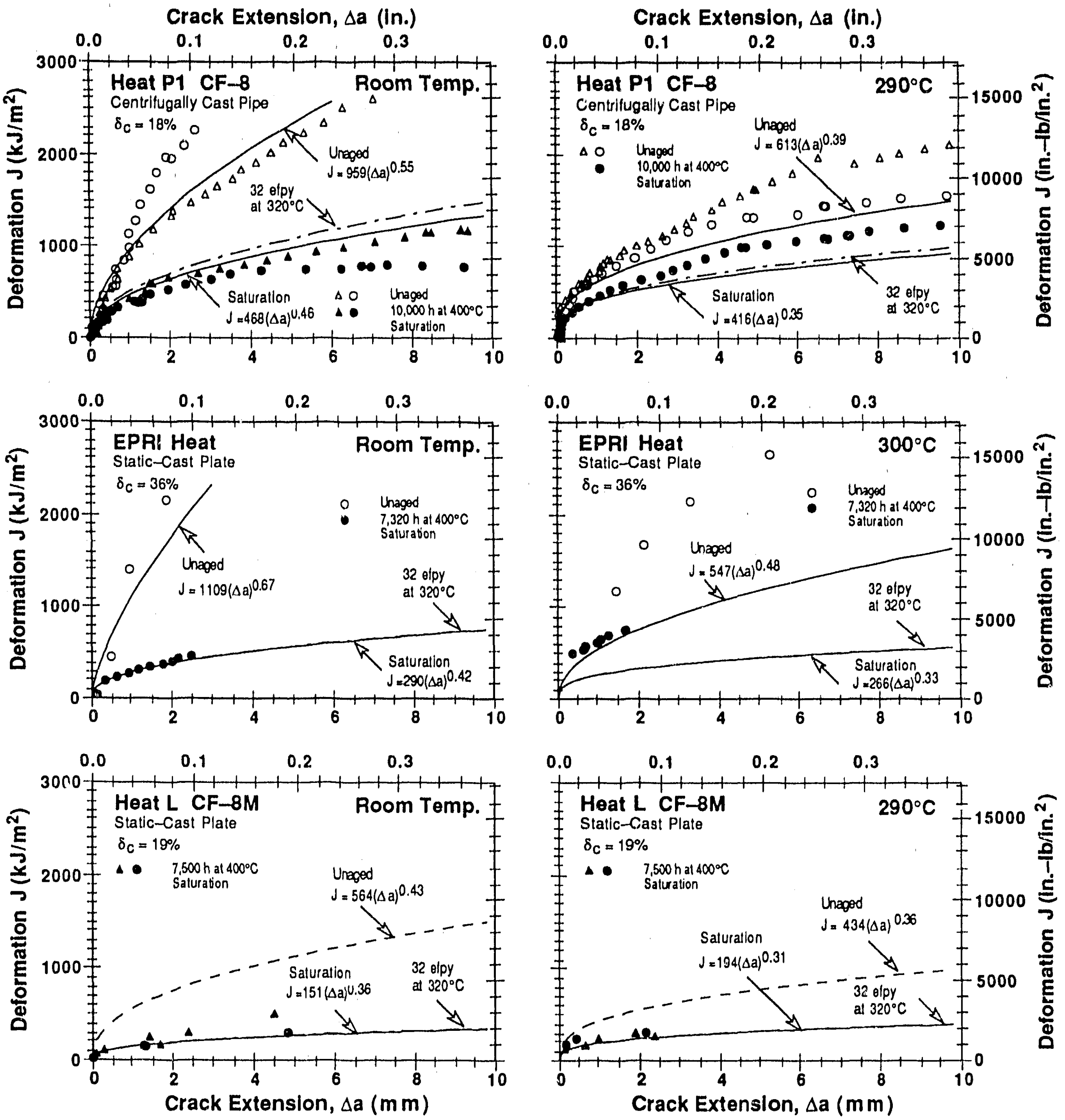

Figure 7. Experimental saturation fracture toughness J–R curves at RT and 290°C and those estimated from the chemical composition of ANL Heat P1, FRA Heat L, and EPRI heat of cast stainless steel. δ_c is the calculated ferrite content.

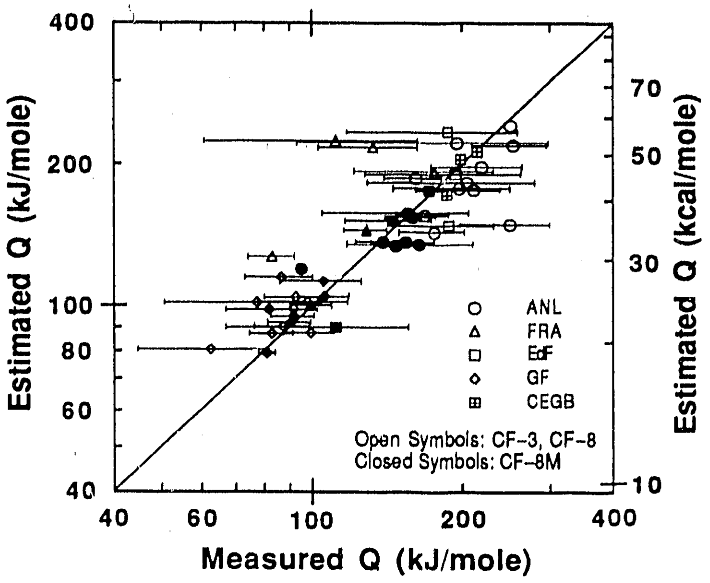

Figure 8. Observed and estimated activation energy for thermal embrittlement

Thermal aging at 400°C is assumed as the baseline aging behavior for a specific material and the aging parameter P is defined by

$$P = \log_{10}[t] - \frac{1000Q}{19.143}\left[\frac{1}{T_s+273} - \frac{1}{673}\right]. \tag{19}$$

The constant β can be determined from Cv_{int} and Cv_{sat}, thus

$$\beta = (\log_{10}Cv_{int} - \log_{10}Cv_{sat})/2. \tag{20}$$

The results for the kinetics of thermal embrittlement indicate that the shape factor α increases linearly with Cv_{sat}. The best fit of the data for the various heats yields

$$\alpha = -0.585 + 0.795\log_{10}Cv_{sat}. \tag{21}$$

Activation energy for thermal embrittlement is expressed in terms of both chemical composition and the constant θ to incorporate the effects of heat treatment and the casting process on the kinetics of thermal embrittlement. The activation energy Q is given by

$$Q = 10\,[74.52 - 7.20\,\theta - 3.46\,Si - 1.78\,Cr - 4.35\,I_1\,Mn + (148 - 125\,I_1)\,N - 61\,I_2\,C], \tag{22}$$

where the indicators $I_1 = 0$ and $I_2 = 1$ for CF-3 or CF-8 steels and assume the values of 1 and 0, respectively, for CF-8M steels. The estimated and observed values of Q for the ANL, FRA, CEGB, and GF heats are plotted in Fig. 8. The predicted values are within the 95% confidence limits for all the heats. Equation 22 is applicable for compositions within ASTM Specification A 351, with an upper limit of 1.2 wt.% for Mn content. Actual Mn content is used up to 1.2 wt.% and is assumed to be 1.2 wt.% for steels containing >1.2 wt.% Mn. Furthermore, the values of Q predicted from Eq. 22 should be between 65 kJ/mole minimum and 250 kJ/mole maximum; Q is assumed to be 65 kJ/mole if the predicted values are lower and 250 kJ/mole if the predicted values are higher.

5.2 Fracture Toughness

The RT Charpy-impact energy of a specific cast stainless steel as a function of service time and temperature can be estimated from estimated Cv_{sat} [Eqs. 1–10] and the kinetics of embrittlement [Eqs. 18–22]. Values of Cv_{int} and the constant θ are required for these estimations. If not known, a typical value of 200 J/cm^2 may be used for Cv_{int}. Parametric studies indicate that the aging response at 280–330°C is relatively insensitive to the value of θ.[19] Varying θ between 2.1 and 3.6 results in almost identical aging behavior at 300°C and differences in aging behavior at 280–330°C are minimal. A median value of 2.9 for θ in Eqs. 18 and 22 can be used to estimate impact energy of cast stainless steel components in service at 280–330°C. With an assumed value of 2.9 for θ, estimations of impact energies before saturation will be nonconservative at service temperatures >330°C for heats with $\theta < 2.9$ and temperatures <280°C for heats with $\theta > 2.9$. To ensure that the estimates are conservative for all materials, a value of 2.5 for θ should be used for temperatures between 330 and 360°C and a value of 3.3 should be used for temperatures <280°C.

The RT Charpy-impact energy observed experimentally and that estimated from the chemical composition and initial impact energy of some of the ANL, FRA, and GF heats aged at temperatures between 290–350°C, are shown in Fig. 9. A θ value of 2.9 was used for the estimations. The estimated change in impact energy at ≤330°C is either accurate or slightly conservative for most of the heats. Even the estimations at 350°C show good agreement with the experimental results because the θ values for the heats shown in the figure are either greater or only slightly lower than 2.9.

The fracture toughness J–R curve for a specific material and aging condition can be obtained by using the estimated RT Charpy-impact energy Cv in Eqs. 18–22. Example of the experimental and estimated J–R curves for a partially aged (i.e., 30,000 h at 320°C) centrifugally cast stainless steel pipe is shown in Fig. 10. The estimated J–R curves show good agreement with the experimental results.

5.3 Tensile Flow Stress

Thermal aging leads to an increase in yield and ultimate stress and a slight decrease in ductility. CF-3 steels show the smallest change and CF-8M steels the largest change in tensile stress. For all grades, the increase in ultimate stress is substantially greater than the increase in yield stress. Some heats show no change in yield stress. Furthermore, specimens aged for short times at high temperatures, e.g., ≈3,000 h at 400°C, often show a decrease in yield and ultimate stresses.

Tensile flow stress of aged cast stainless steels can be estimated from correlations between ratio of the tensile flow stress of aged and unaged cast stainless steels and normalized aging parameter.[20] Flow stress is characterized as the mean of the 0.2% yield and ultimate stresses, and the aging parameter is normalized with respect to a θ value of 2.9. The flow stress ratio $R = (\sigma f_{aged}/\sigma f_{unaged})$ is given by

$$R = a_1 + b_1(P - \theta + 2.9). \qquad (23)$$

Equation 23 is valid for ferrite contents >7% and R values between 1 and a constant c_1. Values of the constants a_1, b_1, and c_1 for different grades of steel and test temperatures are given in Table 3.

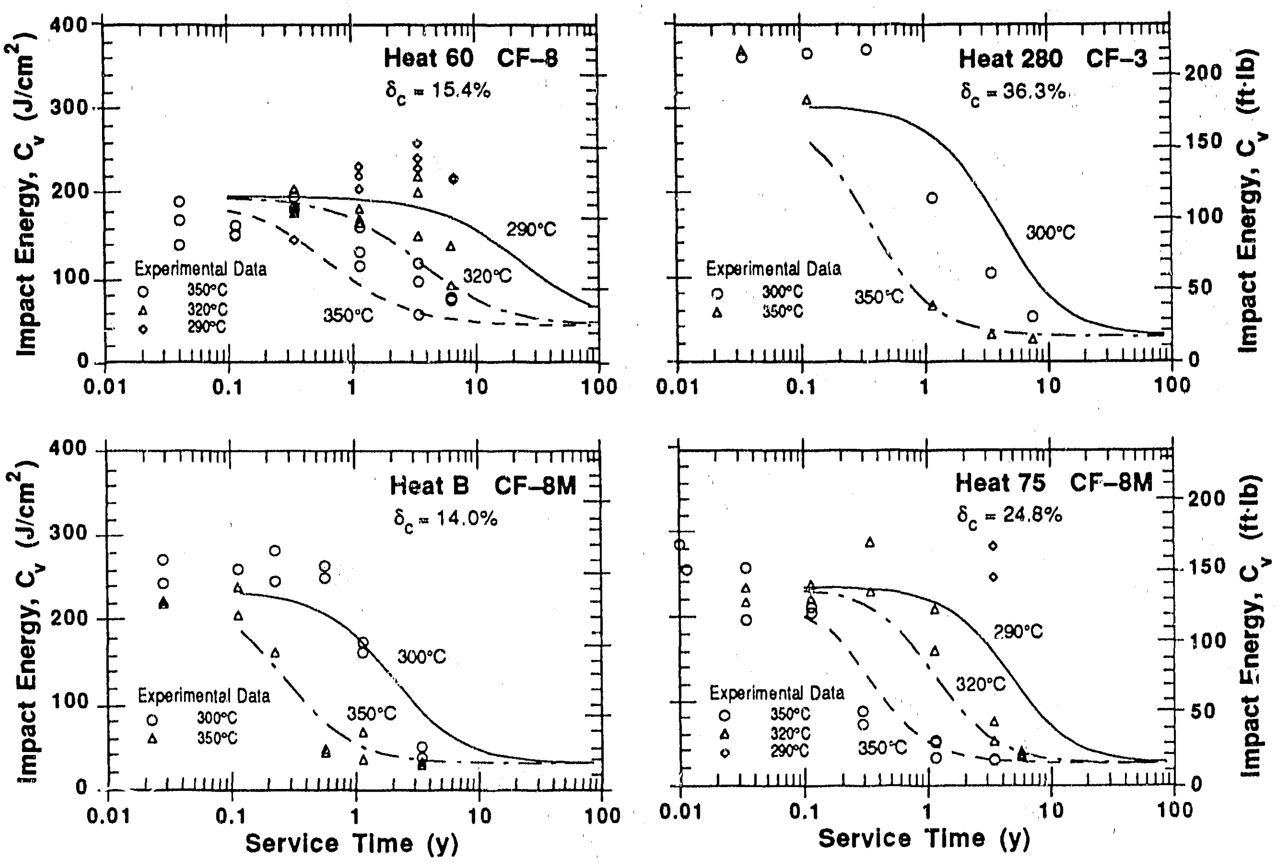

Figure 9. Room-temperature Charpy-impact energy for aged CF-3, CF-8, and CF-8M steels observed experimentally and that estimated from the composition and initial impact energy of the materials from ANL (Heats 60 and 75), FRA (Heat B), and GF (Heat 280) studies. δ_c is the calculated ferrite content.

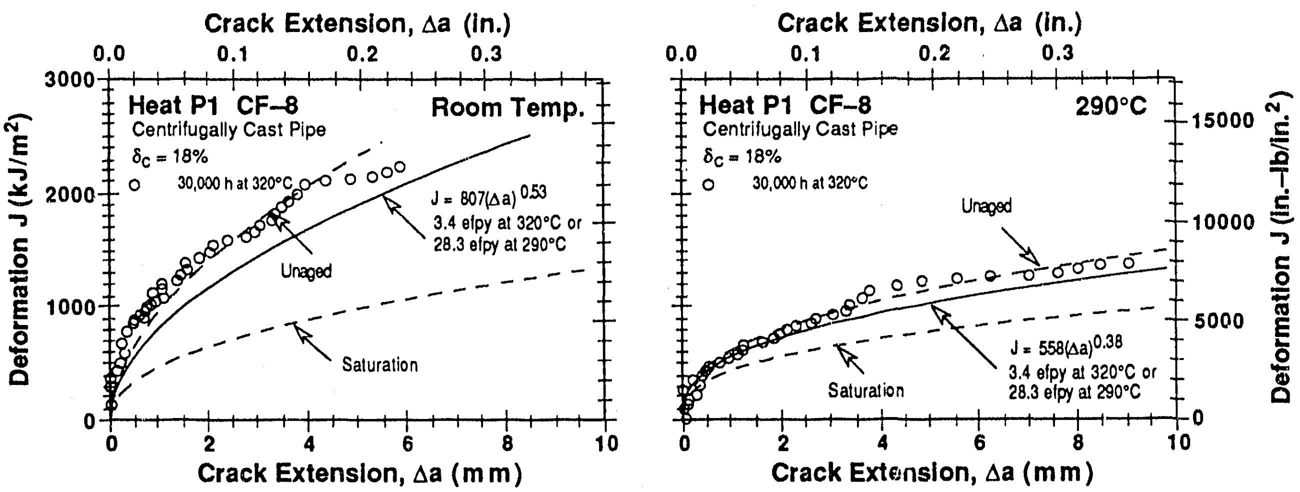

Figure 10. Fracture toughness J–R curve at RT and 290°C, estimated from the chemical composition and initial Charpy-impact energy and determined experimentally for partially aged CF-8 steels. δ_c is the calculated ferrite content.

Table 3. Constants in Eq. 23 for estimating tensile flow stress of aged cast stainless steels

Grade	Room Temp.			290–320°C		
	a_1	b_1	c_1	a_1	b_1	c_1
CF-3	0.94	0.047	1.10	0.89	0.059	1.08
CF-8	0.90	0.074	1.16	0.87	0.088	1.14
CF-8M	0.80	0.101	1.19	0.71	0.143	1.24

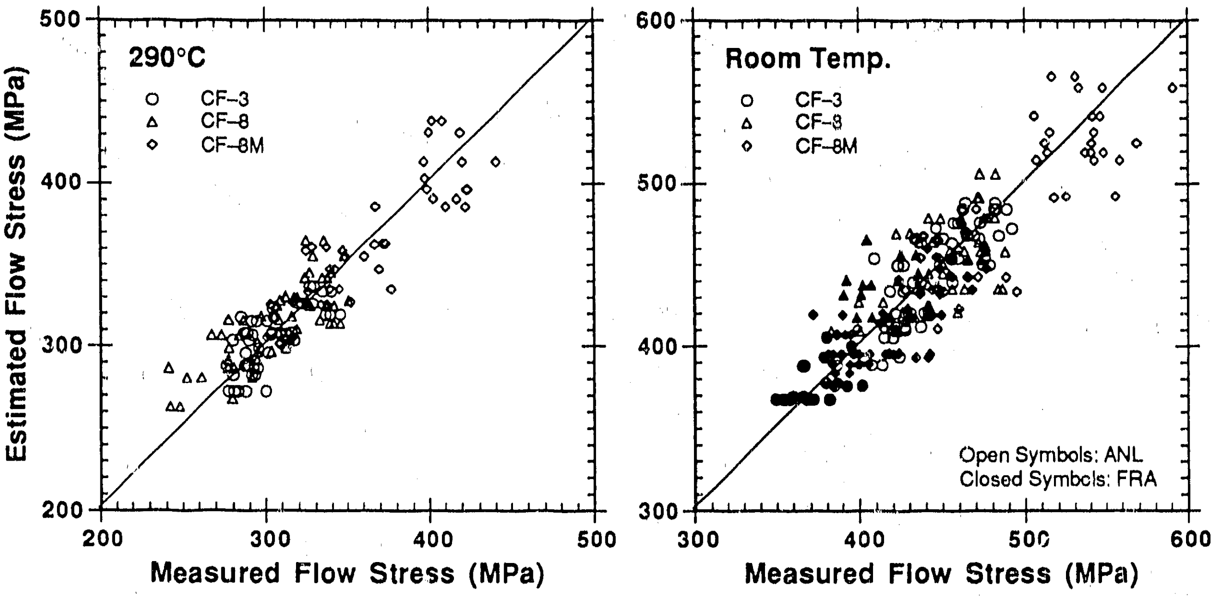

Figure 11. Observed and estimated flow stress of aged cast stainless steel at 290°C and RT

Experimental and estimated tensile flow stress at 290°C and RT for various heats of aged cast stainless steel are shown in Fig. 11. For each heat, the aging parameter was obtained from Eqs. 19 and 22; because most of the data are for aging temperatures ≥350°C, the actual experimental value of θ was used for all the heats. Tensile flow stress was then estimated from Eq. 23 and the initial flow stress of the materials. The estimated values are within 15% of the observed value for most material and aging conditions.

The fracture toughness J_{IC} values for aged cast stainless steels can be determined from the estimated J-R curve and flow stress. The experimental and estimated J_{IC} for the various heats aged at ≤350°C and tested at 290°C and RT are shown in Fig. 12. The chemical composition and the initial Charpy-impact energy and flow stress of the unaged material were used for the estimations. The estimated J_{IC} values show good agreement with the experimental results; for most cases the estimated J_{IC} is lower but within 30% of the observed value.

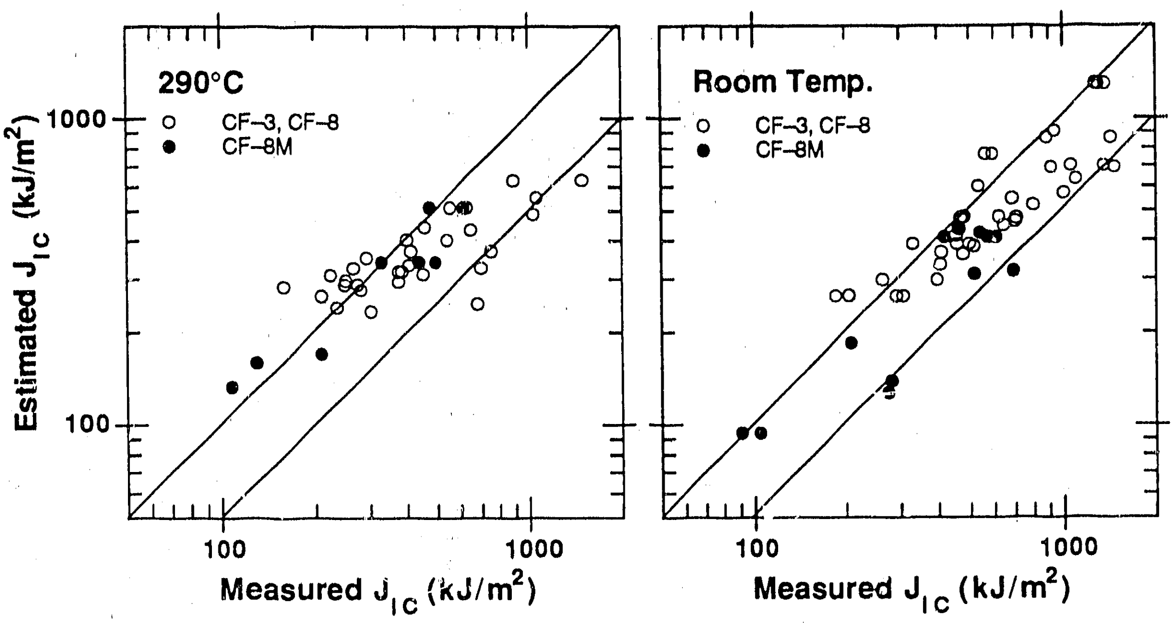

Figure 12. Experimental and estimated values of J_{IC} for aged cast stainless steels at 290°C and RT

6 Conclusions

A procedure and correlations are presented for predicting Charpy–impact energy, tensile flow stress, fracture toughness J–R curve, and J_{IC} value of aged cast stainless steels (ASTM A 351) from known material information. Mechanical properties of a specific cast stainless steel are estimated from the extent and kinetics of thermal embrittlement. Embrittlement of cast stainless steels is characterized in terms of room temperature (RT) Charpy–impact energy. The extent or degree of thermal embrittlement at "saturation," i.e., the minimum impact energy that can be achieved for the material after long–term aging, is determined from chemical composition of the steel. Charpy–impact energy as a function of time and temperature of reactor service is estimated from the kinetics of thermal embrittlement, which is also determined from the chemical composition. The initial impact energy of the unaged steel is required for these estimations. Initial tensile flow stress is needed for estimating the flow stress of the aged material. The fracture toughness J–R curve for the material is then obtained from correlations between RT Charpy–impact energy and fracture toughness parameters. The J_{IC} value is determined from the estimated J–R curve and flow stress. A common "predicted lower–bound" J–R curve for cast stainless steels with unknown chemical composition is also defined for a given grade of steel, range of ferrite content, and temperature. This information can serve as a guideline for establishing the upper limit of ferrite content for a specific grade of steel beyond which thermal aging effects are significant.

Fracture toughness J–R curve data have been mostly obtained on 1–T compact tension specimens. According to ASTM Specification E 1152–87 they are valid only for crack growth up to 10% of the initial uncracked ligament. However, it is widely accepted that the J–R curve crack growth validity limits fall between 25 and 40% of the initial uncracked ligament, or ≈8 mm of crack extension. In future work under this program, these extended validity limits for J–controlled crack growth will be qualified and better defined for cast stainless steels in terms of specimen size, toughness, and crack extension. Representation of J–R curves by expressions other than power law (e.g., by power–exponential relation) will also be evaluated for more accurate extrapolation of J–R curve data.

Acknowledgments

This work was supported by the Office of Nuclear Regulatory Research of the U.S. Nuclear Regulatory Commission. The author thanks A. Sather, T. M. Galvin, L. Y. Bush, W. F. Michaud, and W. F. Burke for experimental contributions and J. Muscara, W. J. Shack, and T. F. Kassner for their helpful discussions.

References

1. O. K. Chopra and H. M. Chung, "Aging Degradation of Cast Stainless Steels: Effects on Mechanical Properties," in *Environmental Degradation of Materials in Nuclear Power Systems–Water Reactors*, G. J. Theus and J. R. Weeks, eds. The Metallurgical Society, Warrendale, PA., pp. 737–748 (1988).
2. O. K. Chopra and H. M. Chung, "Effect of Low-Temperature Aging on the Mechanical Properties of Cast Stainless Steels," in *Properties of Stainless Steels in Elevated Temperature Service*, M. Prager, ed., MPC Vol. 26, PVP Vol. 132, American Society of Mechanical Engineers, New York, pp. 79–105 (1988).
3. O. K. Chopra, "Thermal Aging of Cast Stainless Steels: Mechanisms and Predictions," in *Fatigue, Degradation, and Fracture – 1990*, W. H. Bamford, C. Becht, S. Bhandari, J. D. Gilman, L. A. James, and M. Prager, eds., MPC Vol. 30, PVP Vol. 195, American Society of Mechanical Engineers, New York, pp. 193-214 (1990).
4. O. K. Chopra and A. Sather, *Initial Assessment of the Mechanisms and Significance of Low-Temperature Embrittlement of Cast Stainless Steels in LWR Systems*, NUREG/CR-5385, ANL-89/17, Argonne National Laboratory, Argonne, IL (August 1990).
5. A. Trautwein and W. Gysel, "Influence of Long Time Aging of CF-8 and CF-8M Cast Steel at Temperatures Between 300 and 500°C on the Impact Toughness and the Structure Properties," in *Stainless Steel Castings*, V. G. Behal and A. S. Melilli, eds., ASTM STP 756, pp. 165–189 (1982).
6. E. I. Landerman and W. H. Bamford, "Fracture Toughness and Fatigue Characteristics of Centrifugally Cast Type 316 Stainless Steel Pipe after Simulated Thermal Service Conditions," in *Ductility and Toughness Considerations in Elevated Temperature Service*, MPC-8, American Society of Mechanical Engineers, New York, pp. 99–127 (1978).
7. S. Bonnet, J. Bourgoin, J. Champredonde, D. Guttmann, and M. Guttmann, "Relationship between Evolution of Mechanical Properties of Various Cast Duplex Stainless Steels and Metallurgical and Aging Parameters: An Outline of Current EDF Programmes," *Mater. Sci. and Technol.*, **6**, 221–229 (1990).
8. P. H. Pumphrey and K. N. Akhurst, "Aging Kinetics of CF3 Cast Stainless Steel in Temperature Range 300 – 400°C," *Mater. Sci. and Technol.*, **6**, 211–219 (1990).
9. G. Slama, P. Petrequin, and T. Mager, "Effect of Aging on Mechanical Properties of Austenitic Stainless Steel Castings and Welds," presented at SMIRT Post-Conference Seminar 6, Assuring Structural Integrity of Steel Reactor Pressure Boundary Components, August 29–30, 1983, Monterey, CA.

10. Y. Meyzaud, P. Ould, P. Balladon, M. Bethmont, and P. Soulat, "Tearing Resistance of Aged Cast Austenitic Stainless Steel," presented at Intl. Conf. on Thermal Reactor Safety (NUCSAFE 88), October 1988, Avignon, France.

11. P. McConnell and J. W. Sheckherd, *Fracture Toughness Characterization of Thermally Embrittled Cast Duplex Stainless Steel*, Report NP-5439, Electric Power Research Institute, Palo Alto, CA (September 1987).

12. M. Vrinat, R. Cozar, and Y. Meyzaud, "Precipitated Phases in the Ferrite of Aged Cast Duplex Stainless Steels," *Scripta Metal.*, **20**, 1101-1106 (1986).

13. H. M. Chung and O. K. Chopra, "Long-Term-Aging Embrittlement of Cast Austenitic Stainless Steels - Mechanism and Kinetics," in *Properties of Stainless Steels in Elevated Temperature Service*, M. Prager, ed., MPC Vol. 26, PVP Vol. 132, American Society of Mechanical Engineers, New York, pp. 17-34 (1988).

14. H. M. Chung and T. R. Leax, "Embrittlement of Laboratory and Reactor Aged CF3, CF8, and CF8M Duplex Stainless Steels," *Mater. Sci. and Tech.* **6**, 249-262 (1990).

15. J. Sassen, M. G. Hetherington, T. J. Godfrey, G. D. W. Smith, P. H. Pumphrey, and K. N. Akhurst, "Kinetics of Spinodal Reaction in the Ferrite Phase of a Duplex Stainless Steel," in *Properties of Stainless Steels in Elevated Temperature Service*, M. Prager, ed., MPC Vol. 26, PVP Vol. 132, ASME, New York, pp. 65-78 (1988).

16. M. K. Miller and J. Bentley, "Characterization of Fine-Scale Microstructures in Aged Primary Coolant Pipe Steels," in *Environmental Degradation of Materials in Nuclear Power Systems-Water Reactors*, Proc. 3rd Intl. Symp., G. J. Theus and J. R. Weeks, eds., The Metallurgical Society, Warrendale, PA, pp. 341-349 (1988).

17. P. Auger, F. Danoix, A. Menand, S. Bonnet, J. Bourgoin, and M. Guttmann, "Atom Probe and Transmission Electron Microscopy Study of Aging of Cast Duplex Stainless Steels," *Mater. Sci. and Technol.*, **6**, 301-313 (1990).

18. J. E. Brown, A. Cerezo, T. J. Godfrey, M. G. Hetherington, and G. D. W. Smith, "Quantitative Atom Probe Analysis of Spinodal Reaction in Ferrite Phase of Duplex Stainless Steel," *Mater. Sci. and Technol.*, **6**, 293-300 (1990).

19. O. K. Chopra, *Estimation of Fracture Toughness of Cast Stainless Steels during Thermal Aging in LWR Systems*, NUREG/CR-4513, ANL-90/42, Argonne National Laboratory (June 1991).

20. O. K. Chopra, "Estimation of Fracture Toughness of Cast Stainless Steels in LWR Systems," in *Proc. 19th Water Reactor Safety Information Meeting*, U.S. Nuclear Regulatory Commission (in press, 1992).

21. L. S. Aubrey, P. F. Wieser, W. J. Pollard, and E. A. Schoefer, "Ferrite Measurement and Control in Cast Duplex Stainless Steel," in *Stainless Steel Castings*, V. G. Behal and A. S. Melilli, eds., ASTM STP 756, pp. 126-164 (1982).

22. A. L. Hiser, *Tensile and J-R Curve Characterization of Thermally Aged Cast Stainless Steels*, NUREG/CR-5024, MEA-2229, Materials Engineering Associates, Inc., Lanham, MD, (September 1988).

23. G. E. Hale and S. J. Garwood, "The Effect of Aging on the Fracture Behaviour of Cast Stainless Steel and Weldments," *Mater. Sci. and Technol.*, **6**, pp. 230-235 (1990).

DATE
FILMED
7/27/92